

## Article

# New Sintered Porous Scaffolds of Mg,Sr Co-Substituted Hydroxyapatite Support Growth and Differentiation of Primary Human Osteoblasts In Vitro

Carlo Galli <sup>1,\*</sup>, Elena Landi <sup>2</sup>, Silvana Belletti <sup>1</sup>, Maria Teresa Colangelo <sup>1</sup> and Stefano Guizzardi <sup>1</sup>

<sup>1</sup> Histology and Embryology Lab, DiMeC, Department of Medicine and Surgery, University of Parma, Via Volturmo 39, 43126 Parma, Italy; silvana.belletti@unipr.it (S.B.); mariateresa.colangelo@studenti.unipr.it (M.T.C.); stefano.guizzardi@unipr.it (S.G.)

<sup>2</sup> ISTEC-CNR, Institute of Science and Technology for Ceramics-National Research Council, Via Granarolo 64, 48018 Faenza, Italy; elena.landi@istec.cnr.it

\* Correspondence: carlo.galli@unipr.it; Tel.: +39-0521-906740

**Abstract:** Strontium (Sr) and Magnesium (Mg) are bioactive ions that have been proven to exert a beneficial effect on bone; therefore, their incorporation into bone substitutes has long been viewed as a possible approach to improve tissue integration. However, the thermal instability of Mg-substituted hydroxyapatites has hitherto limited development. We previously described the creation of thermally consolidated porous constructs of Mg,Sr co-substituted apatites with adequate mechanical properties for their clinical use. The present paper describes the biocompatibility of Mg,Sr co-substituted granules using an alveolar-bone-derived primary model of human osteoblasts. Cells were cultured in the presence of different amounts of hydroxyapatite (HA), Sr-substituted HA, or MgSrHA porous macrogranules (with a size of 400–600 microns, obtained by grinding and sieving the sintered scaffolds) for three and seven days, and their viability was measured by a 3-(4,5-dimethylthiazol-2-yl)-2,5-diphenyltetrazolium bromide (MTT) assay. Protein content was measured using the Lowry assay at the same time points. Cell viability was not impaired by any of the tested compounds. Indirect and direct biocompatibility of these macrogranules was assessed by culturing cells in a previously conditioned medium with HA, SrHA, or MgSrHA, or in the presence of material granules. Osteoblasts formed larger and more numerous nodules around SrHA or MgSrHA granules. Furthermore, cell differentiation was evaluated by alkaline phosphatase staining of primary cells cultured in the presence of HA, SrHA, or MgSrHA granules, confirming the increased osteoconductivity of the doped materials.

**Keywords:** strontium-substituted apatite; magnesium-substituted apatite; Mg,Sr co-substituted apatite; primary osteoblasts; biocompatibility



**Citation:** Galli, C.; Landi, E.; Belletti, S.; Colangelo, M.T.; Guizzardi, S. New Sintered Porous Scaffolds of Mg,Sr Co-Substituted Hydroxyapatite Support Growth and Differentiation of Primary Human Osteoblasts In Vitro. *Appl. Sci.* **2021**, *11*, 9723. <https://doi.org/10.3390/app11209723>

Academic Editor: Rossella Bedini

Received: 13 September 2021

Accepted: 13 October 2021

Published: 18 October 2021

**Publisher's Note:** MDPI stays neutral with regard to jurisdictional claims in published maps and institutional affiliations.



**Copyright:** © 2021 by the authors. Licensee MDPI, Basel, Switzerland. This article is an open access article distributed under the terms and conditions of the Creative Commons Attribution (CC BY) license (<https://creativecommons.org/licenses/by/4.0/>).

## 1. Introduction

An effective approach for tissue regeneration is the use of scaffold materials designed to be implanted into the recipient site and support cell ingrowth from neighboring tissues and the deposition of a new extracellular matrix [1]. Synthetic or naturally derived calcium phosphate bioceramics are arguably the most common bone substitutes in the literature and in clinical practice because their composition resembles mineralized bone matrix, though with noteworthy differences [2,3]. Naturally occurring apatite presents numerous substitutions and contains traces of several elements, e.g., Mg and Sr, besides the more abundant Ca and P species [4]. These elements, albeit in small amounts, are important because they affect material properties and perform specific biological activities. Mg<sup>2+</sup>/Ca<sup>2+</sup> balance has been shown to be important in bones because Mg<sup>2+</sup> modulates mineralization by acting as a calcium antagonist [5]. Pre-clinical and clinical studies have reported that Sr enhances bone formation and attenuates bone resorption, thus increasing bone mass

and bone mechanical properties [6,7]. Incorporating these elements into hydroxyapatite (HA) has therefore long appeared as an appealing strategy to increase HA resorbability and improve tissue responses to implantable materials, following a biomimetic approach [8,9]. We have previously reported on the chemical, physical, and in vitro assessment of unfired Mg,Sr-co-substituted HA, and have shown improved performance compared to MgHA [10]. Recently, we have developed a method to produce sintered porous scaffolds of Mg,Sr-enriched hydroxyapatites, thus overcoming the thermal instability of Mg containing HA, and we have characterized them chemically and physically [11]. In the present paper, we proceeded to assess the biocompatibility of these compounds using a primary model of human alveolar bone osteoblasts [12–15]. Furthermore, we investigated whether these materials promote the expression of an osteoblastic phenotype as assessed by the expression of the differentiation marker alkaline phosphatase.

## 2. Materials and Methods

### 2.1. Apatites

Porous 400–600  $\mu\text{m}$  macrogranules were obtained by grinding and sieving sintered porous scaffolds of HA, SrHA, and MgSrHA, the last of which was prepared by Mg ion exchange on sintered SrHA. The scaffolds were prepared by cellulose sponge impregnation; details of the scaffolds preparation and characterization are reported in [11]. Briefly, all the materials were sintered at 1250  $^{\circ}\text{C}$ , have similar porosity networks, are proven to allow for osteoblast cell ingrowth and vascularization, are pure (no secondary phases), and contain about 8% wt Sr and 1.1% wt Mg.

### 2.2. Scanning Electron Microscopy (SEM)

The morphological and microstructural characterization of the macrogranules was performed by environmental scanning electron microscopy (E-SEM FEI Quanta 200, FEI Company, Hillsboro, OR, USA).

### 2.3. Primary Osteoblasts

Human primary osteoblasts were obtained from jawbone specimens harvested during a surgical intervention on a 5-year-old patient and isolated as previously described [16]. Briefly, bone fragments were cleaned from soft tissues remnants, thoroughly rinsed in phosphate-buffered saline (PBS, Sigma Chemicals, St. Louis MO, USA), and then maintained in Dulbecco's Modified Essential Medium (DMEM, Bio Whittaker, Walkersville, MD, USA) enriched with 10% FBS (Foetal Bovine Serum, Bio Whittaker), glutamine (4 mM), streptomycin (100 Ag/mL), and penicillin (100 U/mL) (Penstrep-GibcoBRL, Life Technologies B.V. Breda, The Netherlands) at 37  $^{\circ}\text{C}$  in modified atmosphere (5%  $\text{CO}_2$ , 95% air) until cell outgrowths appeared. Once confluent, cells were detached by trypsin (trypsin-EDTA 0.25%) (Sigma) seeded in Petri dishes (Falcon, Becton Dickinson Europe, Meylan, France), and fed three times a week with DMEM complete medium enriched with fresh ascorbic acid 250  $\mu\text{M}$  [17] to maintain a differentiated osteoblastic phenotype. Cells were further characterized by evaluating alkaline phosphatase activity according to Farley et al. [18] and by osteocalcin production through an ELISA Kit (DAKO s.p.a, Milano, Italy), using a normal skin fibroblast population as a negative control.

### 2.4. Cell Viability Assessment: MTT

Primary osteoblasts were seeded at a concentration of 50,000 cells/mL/well in a 24-well plate. Biomaterial granules were re-suspended in complete DMEM at a concentration of 3 mg/mL and diluted to the desired concentration (3, 1, 0.3, 0.1 mg/mL). One ml of granule suspension was then added to the wells 24 h after seeding, and cells were grown in complete medium for 3 or 7 days. The medium was replaced with fresh solution three times a week. An MTT colorimetric assay, based on the 3-(4,5-dimethylthiazol-2-yl)-2,5-diphenyltetrazolium bromide dye, was performed according to Mosmann [19]. Briefly, 100  $\mu\text{L}$  of MTT substrate at the concentration of 5 mg/mL was added to each well,

and the plate was incubated for 4 h at 37 °C. A solubilization solution was prepared by dissolving a 10% solution of 100X Triton (Sigma Aldrich) in 0.1 N HCl acid isopropanol. One ml solubilization solution was added to each well and incubated for 15 minutes on orbital shaker. Absorbance was then read at 570 nm by a spectrophotometer Infinite F200 microplate reader (Tecan Group Ltd., Männedorf, Switzerland).

### 2.5. Protein Quantitation

Primary osteoblasts were seeded at a concentration of 50,000 cells/mL/well in a 24-well plate. Biomaterial granules were re-suspended in complete DMEM at a concentration 3 mg/mL and diluted to the desired concentration (3, 1, 0.3, 0.1 mg/mL). One ml of granule suspension was then added to the wells 24 h after seeding, and cells were grown in complete medium for 3 or 7 days. Medium was replaced with fresh solution three times a week. Total proteins were then extracted following the Lowry protocol according to Wang and Smith [20]. Briefly, the medium was discarded, the samples were gently rinsed with PBS, and then 200 µL Na-DOC (Sodium Deoxycolate, Sigma Aldrich) in PBS was added and incubated for 1 h on orbital shaker to extract proteins. Two ml Lowry solution/well was then added and incubated for 10 minutes on orbital shaker. Two hundred µL Folin solution (Sigma Aldrich) was added to the samples and incubated for 1 h; the samples were then read at 600 nm with an Infinite F200 microplate reader (Tecan Group Ltd.).

### 2.6. Biocompatibility Assessment: Indirect Test

Fifty thousand cells/mL were seeded in 24-well plates in complete DMEM, and the plates were maintained at 37 °C and 5% CO<sub>2</sub> in a humidified atmosphere for 24 h. Three mg/mL HA, SrHA, or MgSrHA granules was soaked for 24 h in DMEM at 37 °C and 95% humidity, and, as a control, the same volume of DMEM was treated in the same condition. To analyze the effect of the possible release of chemical species from the samples, the supernatant was transferred to culture wells 24 h after seeding; the cells were cultured for 72 h or 7 days. Medium was replaced with fresh solution three times a week. Cells were then observed with inverted microscope (Nikon, Tokyo, Japan), and microphotographs were taken.

### 2.7. Biocompatibility Assessment: Direct Contact Test

Primary osteoblasts were seeded at the concentration of 50,000 cells/mL/well in a 24-well plate. Biomaterial granules were suspended in complete DMEM at a concentration 3 mg/mL and diluted to the concentration of 3 mg/mL. One ml of granule suspension was then added to the wells 24 h after seeding, and cells were grown in complete medium for 72 h or 7 days. Medium was replaced with fresh solution three times a week. Cells were then observed with inverted microscope (Nikon, Tokyo, Japan), and microphotographs were taken.

### 2.8. Alkaline Phosphatase Staining Assay

Primary osteoblasts were seeded at a concentration of 50,000 cells/mL/well in a 24-well plate. Biomaterial granules were suspended in complete DMEM at a concentration of 3 mg/mL and diluted to the concentration of 0.3 mg/mL. One ml of granule suspension was then added to the wells 24 h after seeding, and cells were grown in complete medium for 3 or 7 days. The medium was replaced with fresh solution three times a week. The medium was then discarded, and cells were washed in 0.1 M Cacodylate buffer, fixed in 3% paraformaldehyde in Cacodylate buffer, and then stained as previously described [21]. Briefly, 12 mg Fast Violet B (Sigma-Aldrich) was dissolved in 48 ml distilled water. Two ml Naphthol AS-MX Phosphate Solution (Sigma-Aldrich) was added to the solution, which was then added to the samples for 30 minutes. Samples were then observed with a transmitted light microscope (Nikon, Tokyo, Japan). Stained cells were then quantified using ImageJ software (U.S. National Institutes of Health, Bethesda, MD, USA) on 10 fields per condition. The results were then averaged.

### 2.9. Statistical Analysis

Data were analyzed using Prism 9 (GraphPad, La Jolla, CA, USA). All values are reported as the mean  $\pm$  standard deviation of three repeated experiments. Differences between group means were evaluated with one-way ANOVA statistical test, with Tukey post-test, and differences were considered significant when  $p < 0.05$ .

## 3. Results

### 3.1. SEM Evaluation

When observed with the scanning electron microscope, apatite granules appeared porous, with numerous irregularities and hollow spaces at the micron and sub-micron scale (Figure 1A,B). Figure 1A shows the macrogranules, where parts of the ultramacropore walls (estimated original pore size of over 300  $\mu\text{m}$ ) that characterized the starting MgSrHA scaffold are still visible (see dotted circles), while Figure 1B shows the microstructure of the material, where numerous pores, often interconnected and smaller than 10  $\mu\text{m}$ , are present. At higher magnification, the granule surface appears smooth and regular (Figure 1B). Noteworthy, no evidence of radiation aging was detected on the samples during the experiments.

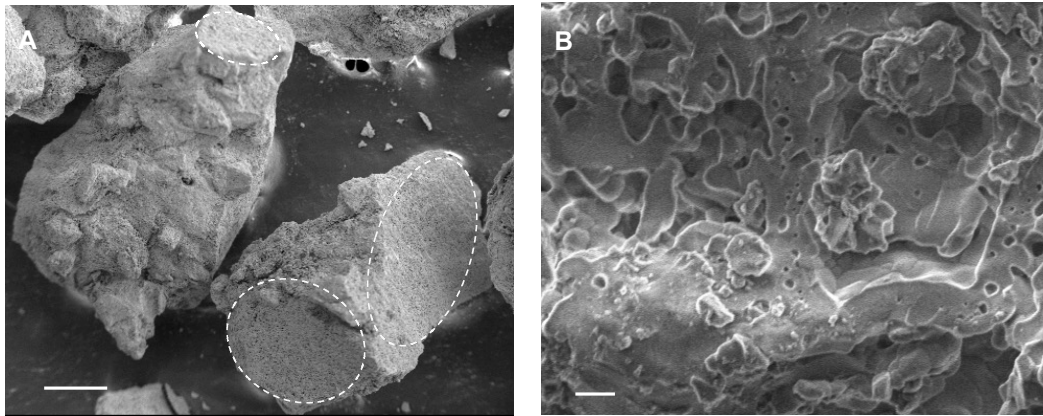


**Figure 1.** Scanning electron microscope microphotographs of MgSrHA granules. The surface displays a high degree of roughness, with numerous cavities, because of the sintering process. Most cavities are a few microns wide, though smaller pores are present. (A) Bar = 200  $\mu\text{m}$ . (B) Bar = 2  $\mu\text{m}$ .

### 3.2. Biocompatibility Assessment

Samples were incubated in complete DMEM for 24 h, which was then added to cell cultures for indirect biocompatibility testing, as recommended in ISO 10993-5 guidelines [22]. The addition of a biomaterial-conditioned medium did not impair cell viability, and no morphological alterations were observed (Figure 2). Cells grew up to confluence and formed well-organized nodules, a typical feature of osteoblast cultures, in all samples, and nodules appeared larger and more numerous in samples conditioned with SrHA (Figure 2C,G) and MgSrHA (Figure 2D,H) granules by day seven.

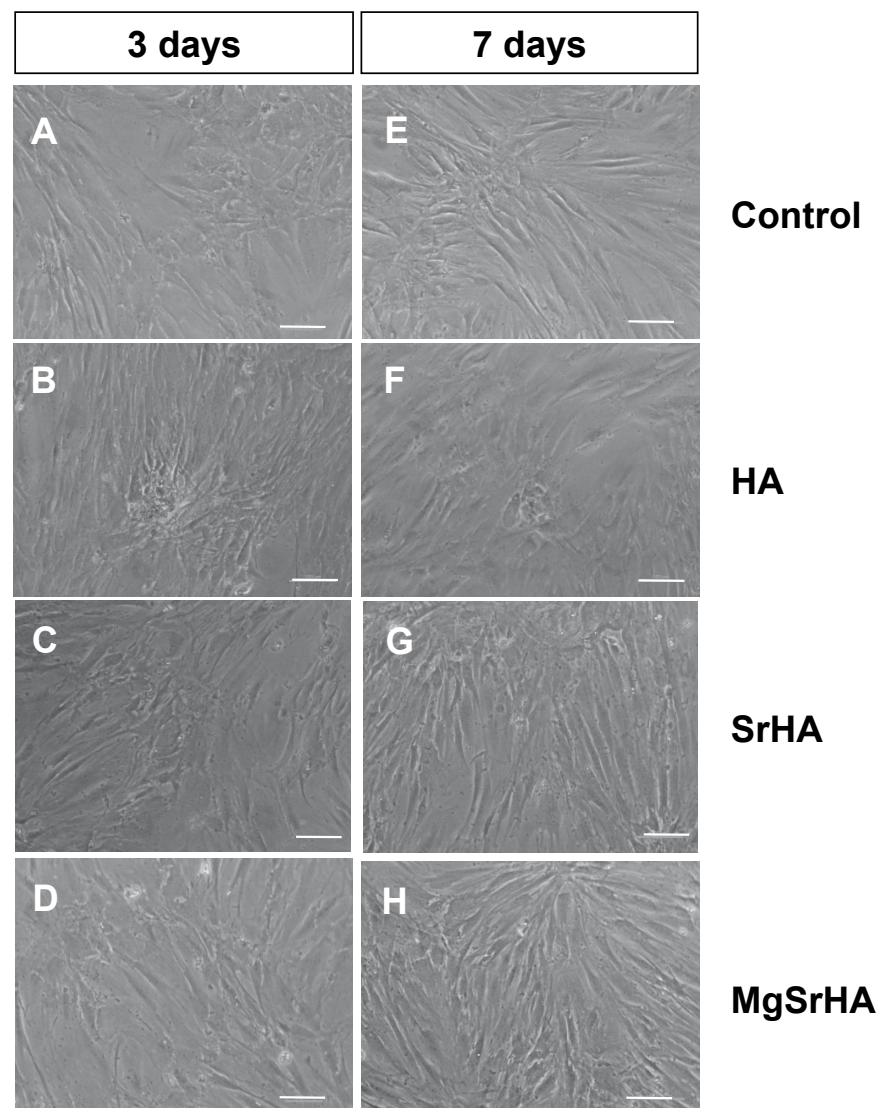


**Figure 2.** Indirect biocompatibility assay: microphotographs of primary human osteoblasts cultured in the presence of (A,E) complete pristine DMEM or previously conditioned with (B,F) hydroxyapatite (HA), (C,G) Sr-substituted HA (SrHA), or (D,H) magnesium, strontium-substituted HA (MgSrHA). Cells were observed at phase contrast after (A–D) three days or (E–H) seven days of culture. Magnification: 10 X. Bar = 20  $\mu$ m.

### 3.3. Cell Viability Assays

To investigate cell viability in the presence of different doses of apatite granules, cells were cultured in the presence of apatite granules for three or seven days (Figure 3). Regardless of their composition, they surrounded the granules of biomaterial (Figure 3), growing in close contact with the apatite. No signs of growth impairment or cell death were observed. Noteworthy, sintered granules consistently released smaller debris scattered over the surface of the culture plate. Cells appeared to grow around or on top of these smaller granules, sometimes forming cell clusters resembling mineralization nodules.

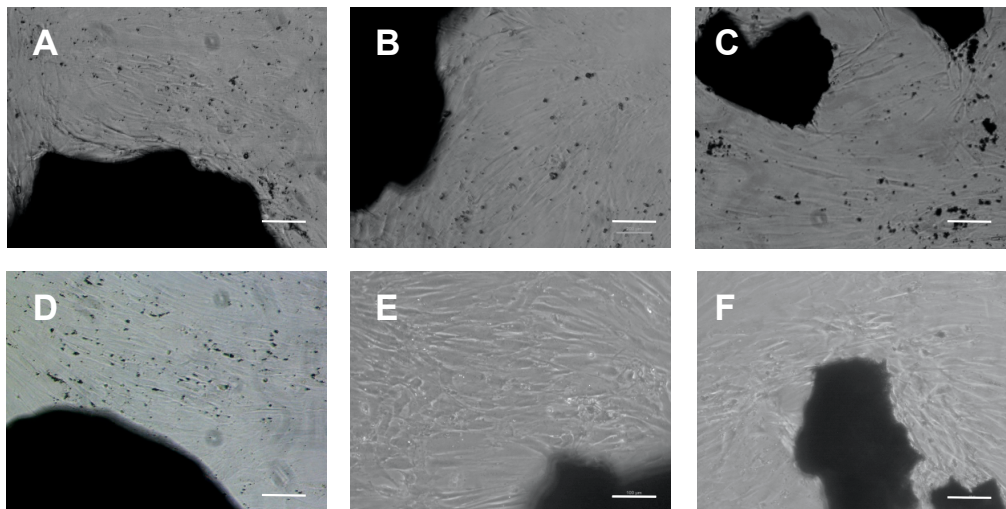


**Figure 3.** Direct biocompatibility assay: microphotographs of primary human osteoblasts cultured in the presence of 3 mg/mL (A,D) hydroxyapatite (HA), (B,E) Sr-substituted HA (SrHA) or (C,F) Magnesium, strontium-substituted HA (MgSrHA) granules. Cells were observed at phase contrast after (A–C) three days or (D–F) seven days of culture. Magnification: 10 X. Bar = 20  $\mu$ m.

To better understand cell kinetics, an MTT assay was performed three and seven days after seeding. Protein content in the culture was also quantified at the same time points (Figure 4). Cells did not exhibit signs of toxicity or impaired growth (data not shown); however, they did not proliferate at an equal rate in all samples (Figure 4). When growing in the presence of HA granules, they tended to grow slower than in the control group, albeit not significantly, regardless of the granule concentration. However, in the presence of 0.1 mg/mL of SrHA granules, their growth rate was significantly slower ( $p < 0.05$ ). In the case of MgSrHA samples, 0.3 mg/mL significantly reduced cell proliferation ( $p < 0.01$ ). When we quantitated protein content in the well, HA significantly increased the amount of protein per well at the concentration of 0.3 mg/mL (Figure 4D). If the concentration of granules increased further, the increment in total proteins decreased. This behavior was not observed with either SrHA or MgSrHA granules. At 0.1 mg/mL of MgSrHA, the rate of protein production was significantly higher than in the control group (Figure 4F).

#### 3.4. Alkaline Phosphatase Staining

Cells were stained for alkaline phosphatase (ALP) in the presence of 0.3 mg/mL apatite granules (Figure 5). Cells displayed a basal level of ALP activity regardless of the culture conditions, as expected in osteoblasts. However, cells cultured in the presence of SrHA or MgSrHA displayed more intense and widespread staining, which became more apparent around and in close contact with biomaterial granules (Figure 5, white arrowheads). No relevant differences were observed between SrHA and MgSrHA samples.

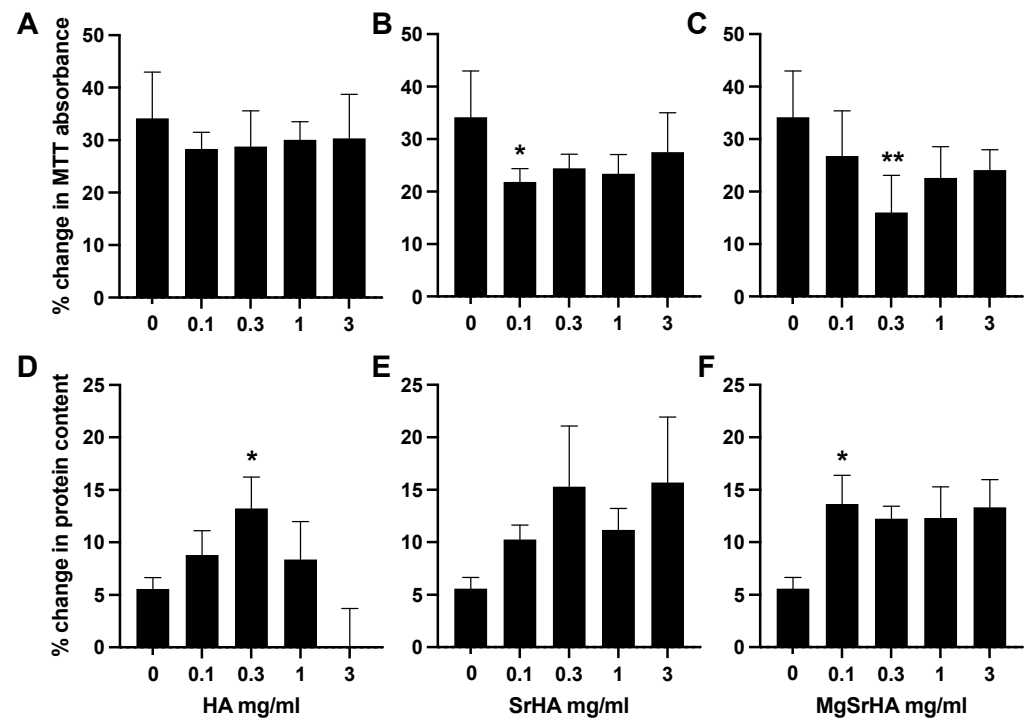


**Figure 4.** Primary human osteoblasts were cultured in the presence of (A,D) hydroxyapatite (HA), (B,E) Sr-substituted HA (SrHA), or (C,F) magnesium, strontium-substituted HA (MgSrHA) granules. Their viability was then measured using MTT assay, and their protein content was assessed with Lowry assay. Graphs (A–C) show the difference in viability levels between day three and day seven, expressed as percent change from day three. Graphs (D–F) show the difference in protein levels between day three and day seven, expressed as percent change from day three. \* =  $p < 0.05$  and \*\* =  $p < 0.01$  vs control.

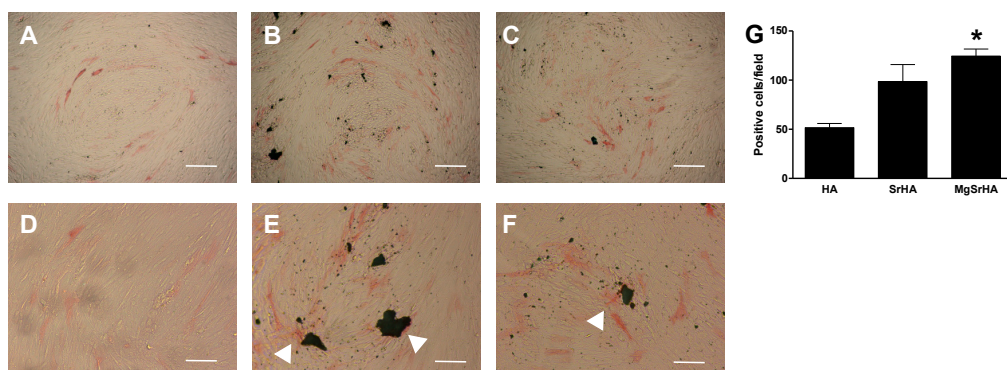


**Figure 5.** (A–F): Alkaline phosphatase (ALP) staining: microphotographs of primary human osteoblasts cultured in the presence of complete DMEM enriched with 0.3 mg/mL (A,D) hydroxyapatite (HA), (B,E) Sr-substituted HA (SrHA) and (C,F) magnesium, strontium-substituted HA (MgSrHA) and stained for ALP (red staining). White arrowheads indicate ALP-positive cells in proximity of material granules. Cells were observed at phase contrast. Magnification: 4 X (A–C), bar = 50  $\mu\text{m}$  or 10 X (D–F), bar = 20  $\mu\text{m}$ . (G) Stained cells were counted and plotted as a bar chart. \* =  $p < 0.05$  vs. HA.

#### 4. Discussion

To properly function within tissues, biomaterials should positively affect cell activity so that they can carry out their physiological role unperturbed, and possibly promote the formation of new tissue, to allow for full integration into the surrounding tissue. In the case of bone substitutes, biomaterials should possess osteoconductive properties, i.e., supporting the formation of new sound bone along their surface. At the very minimum,

biomaterials should be bioinert; i.e., they should not elicit undesired cell responses or exert toxic effects on cells. Biocompatibility assessment is, therefore, an important step when developing novel biomaterials [23,24].

In our previous paper [11], we showed the feasibility of sintered Mg,Sr-substituted hydroxyapatite granular materials, and we characterized their physical and chemical properties. The purpose of the present study was to investigate the response of human primary osteoblasts to these materials. The approach that was followed in this paper was inspired by ISO 10993-5 recommendations, the guidelines that focus on biomaterial cytocompatibility [22], albeit with an important exception. Instead of using cell lines, we decided to resort to primary osteoblasts [16]. These cells were already characterized and used in several studies by our group and were shown to display the expression of differentiation markers and the ability to form mineralization nodules *in vitro* [12,15,25,26]. We believe that such a cell model would increase the transferability of the results to future *in vivo* investigations, as these cells may more closely resemble tissue osteoblasts than immortalized cells.

We therefore proceeded to assess cell viability in the presence of increasing doses of granules. No decrease in cell viability, nor apoptotic cells, was detected in any of the tested samples at any tested concentration, similarly to what was observed with unmodified HA, indicating that the investigated materials did not have toxic effects, as assessed by both MTT assay and protein quantitation. These results were consistent with the literature on HA ceramics, which typically exhibit good cell compatibility [27–29], and with our cell morphological analysis, which revealed that no signs of distress were observed in cells when cultured in the presence of the conditioned medium. This can be easily interpreted as a lack of release of biologically relevant amounts of cytotoxic compounds from the materials.

The MTT data, however, further reveal that cell growth significantly slowed down when cells were cultured with SrHA or MgSrHA, at least at specific concentrations (Figure 4B,C), as opposed to HA samples, in which cells only showed a moderate and non-significant tendency to a decreased proliferation rate (Figure 4A). Noteworthy, a slower proliferation is consistent with an increase in cell differentiation, as it is known that primary osteoblasts gradually lose their duplication potential as they mature. Furthermore, the difference in protein in HA samples vs. SrHA and MgSrHA is not consistent with the increase in cell number unless the Lowry assay is mostly picking up matrix proteins. Taken together, the data in Figure 4 are consistent with an increase in differentiation and matrix deposition in SrHA and MgSrHA samples.

When cultured in the presence of material granules, cells grew along and in close contact with the modified granules, exhibiting similar behavior to what was observed on HA. This behavior is desirable, as cell colonization is the first necessary step for scaffold integration, and the ability of cells to attach and grow along a biomaterial indicates that the biomaterial has promising properties as a scaffold. As composition and surface chemistry have been shown to affect initial cell attachment to biomaterials [30], our findings again point to the high compatibility of the tested granules. Moreover, cells appeared to form a higher number of nodules in the presence of substituted granules (Figure 5), which is a sign of cell differentiation in osteoblast cultures and is again consistent with the MTT and protein results (Figure 4). Interestingly, cell differentiation as assessed by alkaline phosphatase expression was increased in cells growing in contact with substituted HAs (Figure 5). This is compatible with literature showing that Mg and Sr-doped hydroxyapatite and cements increase osteoblast differentiation [31–33]. The increase in ALP expression was observed both along modified granules and all over the culture plate, indicating that the cellular effects were likely to be mediated by the release of bioactive ions into the culture medium. These results provide evidence supporting the potential of these granules for bone regeneration and a rationale to further investigate sintered scaffolds, as outlined in Landi et al. [11].



## 5. Conclusions

Taken together, the present data support the biocompatibility of this material and highlight that MgSrHA sintered granules increase differentiation and matrix formation in primary human osteoblasts and call for further in vivo testing of these materials as improved alternative bone substitutes to stoichiometric HA.

**Author Contributions:** Conceptualization, S.B. and S.G.; methodology, E.L. and M.T.C.; software, C.G.; formal analysis, E.L. and C.G.; investigation, S.B., M.T.C.; resources, E.L., S.G.; writing—original draft preparation, C.G. and E.L.; writing—review and editing, E.L. and S.G.; supervision, S.G.; funding acquisition, C.G. All authors have read and agreed to the published version of the manuscript.

**Funding:** The study was supported through Grant 10-052 from the Osteology Foundation (Basel, Switzerland).

**Institutional Review Board Statement:** Not applicable.

**Informed Consent Statement:** Not applicable.

**Data Availability Statement:** Data are available on request.

**Acknowledgments:** The authors would like to thank Osteology Foundation for the support.

**Conflicts of Interest:** The authors declare no conflict of interest.

## References

1. Cheng, A.; Schwartz, Z.; Kahn, A.; Li, X.; Shao, Z.; Sun, M.; Ao, Y.; Boyan, B.D.; Chen, H. Advances in Porous Scaffold Design for Bone and Cartilage Tissue Engineering and Regeneration. *Tissue Eng. Part B Rev.* **2019**, *25*, 14–29. [[CrossRef](#)]
2. Pereira, H.F.; Cengiz, I.F.; Silva, F.; Reis, R.L.; Oliveira, J.M. Scaffolds and coatings for bone regeneration. *J. Mater. Sci. Mater. Med.* **2020**, *31*, 1–16. [[CrossRef](#)]
3. Bigi, A.; Boanini, E. Functionalized Biomimetic Calcium Phosphates for Bone Tissue Repair. *J. Appl. Biomater. Funct. Mater.* **2017**, *15*, e313–e325. [[CrossRef](#)]
4. Tampieri, A.; Celotti, G.; Landi, E. From biomimetic apatites to biologically inspired composites. *Anal. Bioanal. Chem.* **2005**, *381*, 568–576. [[CrossRef](#)]
5. Li, Y.; Wang, J.; Yue, J.; Wang, Y.; Yang, C.; Cui, Q. High magnesium prevents matrix vesicle-mediated mineralization in human bone marrow-derived mesenchymal stem cells via mitochondrial pathway and autophagy. *Cell Biol. Int.* **2017**, *42*, 205–215. [[CrossRef](#)] [[PubMed](#)]
6. Kołodziejska, B.; Stepień, N.; Kolmas, J. The Influence of Strontium on Bone Tissue Metabolism and Its Application in Osteoporosis Treatment. *Int. J. Mol. Sci.* **2021**, *22*, 6564. [[CrossRef](#)] [[PubMed](#)]
7. Lavet, C.; Mabileau, G.; Chappard, D.; Rizzoli, R.; Ammann, P. Strontium ranelate stimulates trabecular bone formation in a rat tibial bone defect healing process. *Osteoporos. Int.* **2017**, *28*, 3475–3487. [[CrossRef](#)] [[PubMed](#)]
8. Okuzu, Y.; Fujibayashi, S.; Yamaguchi, S.; Yamamoto, K.; Shimizu, T.; Sono, T.; Goto, K.; Otsuki, B.; Matsushita, T.; Kokubo, T.; et al. Strontium and magnesium ions released from bioactive titanium metal promote early bone bonding in a rabbit implant model. *Acta Biomater.* **2017**, *63*, 383–392. [[CrossRef](#)] [[PubMed](#)]
9. Sartori, M.; Giavaresi, G.; Tschon, M.; Martini, L.; Dolcini, L.; Fiorini, M.; Pressato, D.; Fini, M. Long-term in vivo experimental investigations on magnesium doped hydroxyapatite bone substitutes. *J. Mater. Sci. Mater. Electron.* **2014**, *25*, 1495–1504. [[CrossRef](#)] [[PubMed](#)]
10. Landi, E.; Uggeri, J.; Medri, V.; Guizzardi, S. Sr, Mg cosubstituted HA porous macro-granules: Potentialities as resorbable bone filler with antiosteoporotic functions. *J. Biomed. Mater. Res. Part A* **2013**, *101A*, 2481–2490. [[CrossRef](#)]
11. Landi, E.; Guizzardi, S.; Papa, E.; Galli, C. Mg,Sr-Cosubstituted Hydroxyapatite with Improved Structural Properties. *Appl. Sci.* **2021**, *11*, 4930. [[CrossRef](#)]
12. Galli, C.; Guizzardi, S.; Passeri, G.; Martini, D.; Tinti, A.; Mauro, G.; Macaluso, G.M. Comparison of Human Mandibular Osteoblasts Grown on Two Commercially Available Titanium Implant Surfaces. *J. Periodontol.* **2005**, *76*, 364–372. [[CrossRef](#)] [[PubMed](#)]
13. Passeri, G.; Cacchioli, A.; Ravanetti, F.; Galli, C.; Elezi, E.; Macaluso, G.M. Adhesion pattern and growth of primary human osteoblastic cells on five commercially available titanium surfaces. *Clin. Oral Implant. Res.* **2010**, *21*, 756–765. [[CrossRef](#)] [[PubMed](#)]
14. Guizzardi, S.; Galli, C.; Martini, D.; Belletti, S.; Tinti, A.; Raspanti, M.; Taddei, P.; Ruggeri, A.; Scandroglio, R. Different Titanium Surface Treatment Influences Human Mandibular Osteoblast Response. *J. Periodontol.* **2004**, *75*, 273–282. [[CrossRef](#)] [[PubMed](#)]
15. Galli, C.; Macaluso, G.M.; Guizzardi, S.; Vescovini, R.; Passeri, M.; Passeri, G. Osteoprotegerin and Receptor Activator of Nuclear Factor-Kappa B Ligand Modulation by Enamel Matrix Derivative in Human Alveolar Osteoblasts. *J. Periodontol.* **2006**, *77*, 1223–1228. [[CrossRef](#)]

16. Gallagher, J.A.; Gundle, R.; Beresford, J.N.; Jones, G.E. Isolation and Culture of Bone-Forming Cells (Osteoblasts) from Human. *Bone* **2003**, *2*, 233–262. [[CrossRef](#)]
17. Beresford, J.; Gallagher, J.; Poser, J.; Russell, R.G.G. Production of osteocalcin by human bone cells in vitro. Effects of 1,25(OH)<sub>2</sub>D<sub>3</sub>, 24,25(OH)<sub>2</sub>D<sub>3</sub>, parathyroid hormone, and glucocorticoids. *Metab. Bone Dis. Relat. Res.* **1984**, *5*, 229–234. [[CrossRef](#)]
18. Farley, J.R.; Hall, S.L.; Tanner, M.A.; Wergedal, J.E. Specific activity of skeletal alkaline phosphatase in human osteoblast-line cells regulated by phosphate, phosphate esters, and phosphate analogs and release of alkaline phosphatase activity inversely regulated by calcium. *J Bone Miner Res.* **1994**, *9*, 497–508. [[CrossRef](#)]
19. Mosmann, T. Rapid colorimetric assay for cellular growth and survival: Application to proliferation and cytotoxicity assays. *J. Immunol. Methods* **1983**, *65*, 55–63. [[CrossRef](#)]
20. Wang, C.-S.; Smith, R.L. Lowry determination of protein in the presence of Triton X-100. *Anal. Biochem.* **1975**, *63*, 414–417. [[CrossRef](#)]
21. Ziomek, C.A.; Lepire, M.L.; Torres, I. A highly fluorescent simultaneous azo dye technique for demonstration of nonspecific alkaline phosphatase activity. *J. Histochem. Cytochem.* **1990**, *38*, 437–442. [[CrossRef](#)]
22. ISO 10993-5. *Biological Evaluation of Medical Devices—Part 5: Tests for Cytotoxicity: In vitro Methods*, 3rd ed.; ISO: Geneva, Switzerland, 2009.
23. Fini, M.; Giardino, R. In vitro and in vivo tests for the biological evaluation of candidate orthopedic materials: Benefits and limits. *J. Appl. Biomater. Biomech.* **2010**, *1*, 155–163.
24. Torricelli, P.; Fini, M.; Giavaresi, G.; Giardino, R. In vitro Models to Test Orthopedic Biomaterials in View of Their Clinical Application in Osteoporotic Bone. *Int. J. Artif. Organs* **2004**, *27*, 658–663. [[CrossRef](#)]
25. Gatti, R.; Orlandini, G.; Uggeri, J.; Belletti, S.; Galli, C.; Raspanti, M.; Scandroglio, R.; Guizzardi, S. Analysis of living cells grown on different titanium surfaces by time-lapse confocal microscopy. *Micron* **2006**, *39*, 137–143. [[CrossRef](#)]
26. Guizzardi, S.; Galli, C.; Govoni, P.; Boratto, R.; Cattarini, G.; Martini, D.; Belletti, S.; Scandroglio, R. Polydeoxyribonucleotide (PDRN) promotes human osteoblast proliferation: A new proposal for bone tissue repair. *Life Sci.* **2003**, *73*, 1973–1983. [[CrossRef](#)]
27. Matsushima, A.; Kotobuki, N.; Tadokoro, M.; Kawate, K.; Yajima, H.; Takakura, Y.; Ohgushi, H. In Vivo Osteogenic Capability of Human Mesenchymal Cells Cultured on Hydroxyapatite and on  $\beta$ -Tricalcium Phosphate. *Artif. Organs* **2009**, *33*, 474–481. [[CrossRef](#)] [[PubMed](#)]
28. Okamoto, M.; Dohi, Y.; Ohgushi, H.; Shimaoka, H.; Ikeuchi, M.; Matsushima, A.; Yonemasu, K.; Hosoi, H. Influence of the porosity of hydroxyapatite ceramics on in vitro and in vivo bone formation by cultured rat bone marrow stromal cells. *J. Mater. Sci. Mater. Electron.* **2006**, *17*, 327–336. [[CrossRef](#)] [[PubMed](#)]
29. Bernhardt, A.; Lode, A.; Peters, F.; Gelinsky, M. Novel ceramic bone replacement material Osbone® in a comparative in vitro study with osteoblasts. *Clin. Oral Implant. Res.* **2011**, *22*, 651–657. [[CrossRef](#)] [[PubMed](#)]
30. Hutmacher, D.W. Scaffolds in tissue engineering bone and cartilage. *Biomaterials* **2000**, *21*, 2529–2543. [[CrossRef](#)]
31. Gao, J.; Wang, M.; Shi, C.; Wang, L.; Wang, D.; Zhu, Y. Synthesis of trace element Si and Sr codoping hydroxyapatite with non-cytotoxicity and enhanced cell proliferation and differentiation. *Biol. Trace Element Res.* **2016**, *174*, 208–217. [[CrossRef](#)]
32. Singh, S.S.; Roy, A.; Lee, B.; Parekh, S.; Kumta, P.N. Murine osteoblastic and osteoclastic differentiation on strontium releasing hydroxyapatite forming cements. *Mater. Sci. Eng. C* **2016**, *63*, 429–438. [[CrossRef](#)] [[PubMed](#)]
33. Yin, P.; Feng, F.F.; Lei, T.; Zhong, X.H.; Jian, X.C. Osteoblastic cell response on biphasic fluorhydroxyapatite/strontium-substituted hydroxyapatite coatings. *J. Biomed. Mater. Res. Part A* **2013**, *102*, 621–627. [[CrossRef](#)] [[PubMed](#)]